

Regge-Pole Model for pp and $\bar{p}p$ Elastic Scattering at High Energies

DONALD M. AUSTIN, WILLIAM H. GREIMAN, AND WILLIAM RARITA
Lawrence Radiation Laboratory, University of California, Berkeley, California 94720
 (Received 26 June 1970)

High-energy data for pp and $\bar{p}p$ elastic scattering are confronted with the simple Regge-pole model in an attempt to discover which features of these data, if any, are beyond the power of this model. The simplest representation, with only three poles (P , P' , and ω), gives a reasonable fit to all the data except the "dip" structure in the $\bar{p}p$ differential cross sections (DCS). Several types of parametrizations were tested, including various ghost-eliminating mechanisms, and all produced comparable fits. To account for the $\bar{p}p$ DCS structure, and simultaneously circumvent the factorization difficulties caused by the universal zero in the ω amplitude, a fourth pole (the ω') was introduced. The four-pole parametrizations (several were tested) provide adequate fits to all the data, including the $\bar{p}p$ DCS structure, and in addition come much closer to satisfying the sum-rule constraints imposed, through factorization, by the πN and KN analyses. For completeness, another vacuum-type pole (the P'') is introduced and five-pole fits parametrized as in cut models are compared with pure pole models. The results are somewhat ambiguous, showing that the high-energy differential and total cross sections, polarization, ratio of real to imaginary part, and Serpukhov slope data all together are still not sufficient for determining the differences between many possible parametrizations.

I. INTRODUCTION

SEVERAL recent experiments on proton-proton and antiproton-proton elastic scattering indicate some new features of these reactions which were not predicted very accurately by previous Regge-pole fits.¹ Among the features requiring modification of the old fits are the positive polarization near the forward direction for both reactions, the high-energy total cross section and slope measurements from Serpukhov, and the structure in the differential cross sections (DCS) seen for $-t \approx 0.6$ (GeV/c)² (see Sec. II for references). Many authors have obtained fits to some of these features by introducing absorptive cuts or other modifications of simple Regge-pole theory. It is our purpose here to investigate precisely which features of the data, if any, are not amenable to the simple Regge-pole representation of the scattering amplitudes. To this end, we have attempted several parametrizations conforming to the criteria of simple Regge-pole theory—i.e., parameters restricted to the more or less accepted values associated with the trajectory and residue functions established by previous analyses considering finite-energy and continuous-moment sum rules (FESR and CMSR), the resonance spectrum, and factorization.

In Sec. II we describe the data used in the analysis, and Sec. III gives a brief description of our parametrization of the amplitudes and observables. Section IV is devoted to fits using only the three well-known isoscalar Regge trajectories P , P' , and ω , which give an adequate description of most of the data, but seem incapable of describing some important features. In Sec. V we attempt to improve the fits as well as circumvent the factorization difficulties of the ω residue function by introducing a secondary ω -type contribution with several different parametrizations. The rather

ambiguous results obtained from this process lead us to Sec. VI, where all caution is abandoned and five-pole fits are investigated. The five-pole parametrizations are seen to provide excellent fits to all the data, including the structure seen in the latest experiments, with reasonable but nonunique values of the parameters. The discussion of the significance of the various fits is pursued in Sec. VII.

II. DESCRIPTION OF DATA

A. Cross-Section Data

Several interesting experiments done since the RRCP fits¹ invite a new interpretation of the structure seen in elastic $N-N$ cross-section data. Of particular interest are the $\bar{p}p$ total cross sections² and the slope measurements of the pp DCS,³ which extend the lab momentum range under consideration to 70 GeV/c. This wide range of lab momentum allows much more precision in the determination of the energy dependence and, therefore, the Regge trajectories. Some high-precision DCS data which show interesting structure in the Regge region have become available recently. The $\bar{p}p$ DCS at⁴ 8.0 and 16.0 GeV/c indicate a shoulder, or the remnants of a dip occurring at lower energies, near $-t = 0.6$ (GeV/c)². New pp DCS data at⁵ 19.2 and

² J. V. Allaby, Yu. B. Bushnin, S. P. Denisov, A. N. Diddens, R. W. Dobinson, S. V. Donskov, G. Giacomelli, Yu. P. Gorin, A. Klovning, A. I. Petrukhin, Yu. D. Prokoshkin, R. S. Shuvalov, C. A. Stahlbrand, and D. A. Stoyanova, *Phys. Letters* **30B**, 500 (1969).

³ G. G. Beznogikh, A. Buyak, K. I. Iovchev, L. F. Kirillova, P. K. Markov, B. A. Morozov, V. A. Nikitin, P. V. Nomokonov, M. G. Shafranov, V. A. Sviridov, Troung Bien, V. I. Zayachki, N. K. Zhidkov, L. S. Zolin, S. B. Nurusev, and V. L. Solovianov, *Phys. Letters* **30B**, 274 (1969).

⁴ D. Birnbaum, R. M. Edelstein, N. C. Hien, T. J. McMahon, J. F. Mucci, J. S. Russ, E. W. Anderson, E. J. Bleser, H. R. Blüden, G. B. Collins, D. Garelick, J. Menes, and F. Turkot, *Phys. Rev. Letters* **23**, 663 (1969).

⁵ J. V. Allaby, F. Binon, A. N. Diddens, P. Duteil, A. Klovning, R. Meunier, J. P. Peigneux, E. J. Sacharidis, K. Schlupmann, M. Spighele, J. P. Street, A. M. Thorndike, and A. M. Wetherell, *Phys. Letters* **28B**, 67 (1968).

¹ William Rarita, Robert J. Riddell, Charles B. Chiu, and Roger J. N. Phillips, *Phys. Rev.* **165**, 1615 (1967), hereafter referred to as RRCP.

21.1 GeV/c show a definite flattening effect for $-t > 1.0$ (GeV/c)². These two features pose severe constraints on the residue functions.

B. Polarization Data

Perhaps the most interesting of the new data are the polarization data at 6.0 GeV/c for pp and $\bar{p}p$,⁶ and the 14.0-GeV/c data for pp .⁷ The precision of these new data is critical for determining structure of residue functions, such as the sign of the helicity-flip terms and ghost-eliminating mechanisms.

The 6.0-GeV/c pp polarization has distinctive dips near $-t=0.6$ and 0.9 (GeV/c)², and a large ($\approx 25\%$) bump near $-t=1.25$ (GeV/c)². The 14.0-GeV/c data, on the other hand, dip to $\approx -10\%$ at $-t=1.25$ (GeV/c)², indicating a rather drastic energy dependence at large $-t$ that places severe constraints on the parameters. Also, since the $\bar{p}p$ polarization at 6.0 GeV/c is positive for $-t < 0.3$ (GeV/c)², the mechanism producing this polarization cannot be P - ω interference, as previously conjectured,¹ since the pp and $\bar{p}p$ data have the same sign for small $-t$ and, moreover, do not vanish at the crossover point, $-t \approx 0.13$ (GeV/c)².

C. Ratio of Real to Imaginary Part and Slope Data

The data on the ratio of the real to the imaginary part of the forward scattering amplitude, taken as a whole, are inconsistent. Rather than favor one experiment over another or attempt to juggle systematic errors, we simply used the data as published. This means that a χ^2 of 3 or 4 per point is the best one can expect for a fit. Our fits reflect this fact, while producing reasonable agreement with the over-all trend of the data to decrease in magnitude with increasing energy.

The pp DCS slope data³ were taken in the range $0.008 \leq -t \leq 0.12$ (GeV/c)², for p_{lab} from 13.0 to 69.9 GeV/c. Since these data do not coincide with the other DCS data in this energy range,⁸ we scaled the data by the systematic error quoted by the experimenters: ± 0.3 (actually, we multiplied the data by a scale factor of 0.97, which amounts to very nearly the same thing). With the exception of the point at $p_{\text{lab}} = 63.5$ GeV/c, which is somewhat higher than the other points and invariably produced a χ^2 of 10 to 20, we were able to obtain fits with a χ^2 of 1 per point or so with nearly all parametrizations. Hence, our belief is that these

⁶ M. Borghini, L. Dick, L. di Lella, A. Navarro, J. C. Olivier, K. Reibel, G. Coignet, D. Cronenberger, G. Gregoire, K. Kuroda, A. Michalowicz, M. Poulet, D. Sillou, C. Bellettini, P. L. Barccini, T. Del Prette, L. Foa, G. Sanguinetti, and M. Valdata, Phys. Letters **31B**, 405 (1970).

⁷ R. T. Bell, M. Borghini, L. Dick, G. Gregoire, L. di Lella, J. C. Olivier, M. Poulet, P. Scharff-Hansen, D. Cronenberger, K. Kuroda, A. Michalowicz, G. Bellettini, P. L. Braccini, T. Del Prette, L. Foa, G. Sanguinetti, and M. Valdata, in *Proceedings of the Fourteenth International Conference on High-Energy Physics, Vienna, 1968*, edited by J. Prentki and J. Steinberger (CERN, Geneva, 1968).

⁸ R. A. Carrigan, Jr., Phys. Rev. Letters **24**, 168 (1970).

data produced little difficulty for the Regge-pole representation of the scattering amplitudes. As for determining the slope of the Pommeranchukon trajectory, it is very important to consider the range of energy involved as well as the aberrations of the data. For example, if one takes the two points at $p_{\text{lab}} = 27.5$ and 69.9 GeV/c, one finds

$$\alpha_{P'} = \frac{\Delta(\text{slope})}{2 \ln(s_2/s_1)} = 0.33 \text{ (GeV/c)}^{-2};$$

selecting the two points at $p_{\text{lab}} = 13.0$ and 63.5 GeV/c gives $\alpha_{P'} = 0.7$ (GeV/c)⁻². Although the first value appears to have been determined in a more reasonable manner, one should be hesitant about ignoring other choices. The data are simply not good enough to decide such fine points.

D. Summary

Table I summarizes our selection of data used in the fits.⁹⁻¹⁸

III. KINEMATICS AND NOTATION

Our notation is adapted from RRCP,¹ with a few minor changes. Only terms of first order in $\cos\theta_t$ have been kept, and we parametrize the t -channel helicity amplitudes and use them directly in the expressions for observables. Ignoring unnatural parity contributions, such as π , A_1 , etc., we find three t -channel helicity amplitudes (free of kinematic singularities and parity conserving) which we parametrize as follows:

$$\Phi_1 = \Phi_2 = \sum_i \xi_i f_{s_s}^i(t) \nu^{\alpha_i(t)},$$

$$\Phi_3 = -\Phi_4 = -\sum_i \xi_i f_{n_n}^i(t) \nu^{\alpha_i(t)},$$

$$\Phi_5 = \sum_i \xi_i f_{s_n}^i(t) \nu^{\alpha_i(t)},$$

⁹ Most of these data are included in semiretrievable form in the compendium by Geoffrey C. Fox and Chris Quigg, LRL Report No. UCRL-20001, 1970 (unpublished).

¹⁰ K. J. Foley, S. J. Lindenbaum, W. A. Love, S. Ozaki, J. J. Russel, and L. C. L. Yuan, Phys. Rev. Letters **11**, 425 (1963); **11**, 503 (1963); **15**, 45 (1965).

¹¹ W. Galbraith, E. W. Jenkins, T. F. Kycia, B. A. Leontic, R. H. Phillips, A. L. Read, and R. Rubenstein, Phys. Rev. **138**, B913 (1965).

¹² K. J. Foley, R. S. Jones, S. J. Lindenbaum, W. A. Love, S. Ozaki, E. D. Platner, C. A. Quarles, and E. H. Willen, Phys. Rev. Letters **19**, 857 (1967).

¹³ G. Bellettini, G. Cocconi, A. N. Diddens, E. Lillothun, J. Pahl, J. P. Scanlon, J. Walters, A. M. Wetherell, and P. Zanella, Phys. Letters **14**, 164 (1965).

¹⁴ P. Grannis, J. Arens, O. Chamberlain, B. Dieterle, C. Shultz, G. Shapiro, H. Steiner, L. Van Rossum, and D. Weldon, Phys. Rev. **148**, 1297 (1966).

¹⁵ M. Borghini, G. Coignet, L. Dick, K. Kuroda, L. di Lella, P. C. Macq, A. Michalowicz, and J. C. Olivier, Phys. Letters **24B**, 77 (1966).

¹⁶ E. Lohrmann, H. Meyer, and H. Winzler, Phys. Letters **13**, 78 (1964).

¹⁷ A. E. Taylor, A. Ashmore, W. S. Chapman, D. F. Falla, W. H. Range, D. B. Scott, A. Astbury, F. Copocci, and T. G. Walker, Phys. Letters **14**, 54 (1965).

¹⁸ G. Bellettini, G. Cocconi, A. N. Diddens, E. Lillothun, J. P. Scanlon, and A. M. Wetherell, Phys. Letters **19**, 705 (1966).

TABLE I. Data used in the fits. (See Ref. 9.)

	p_{lab}
$d\sigma/dt$ (238 points)	
$p\bar{p}$	6.8, 8.8, 10.8, 12.8, 14.8, 16.7, 19.6, 21.9, 24.6 ^a ; 19.2, 21.1 ^b ;
$\bar{p}p$	7.2, 8.9, 10.0, 11.8, 12.0 ^c ; 8.0, 16.0 ^c ;
σ_T (28 points)	
$p\bar{p}$	6.0–22.0, ^d 7.8–26.0, ^e 10.1, 19.3, 26.4 ^f ;
$\bar{p}p$	6.0–22.0, ^d 20.0–50.0 ^g ;
Polarization (99 points)	
$p\bar{p}$	5.9, 7.0 ^h , 6.0, ⁱ 10.0, 12.0, ^j 14.0 ^k ;
$\bar{p}p$	6.0 ^l ;
Re/Im ¹ (15 points)	
$p\bar{p}$	7.8–26.2, ^e 10.1, 19.3, 26.4, ^f 24.0, ^m 7.85, ⁿ 10.0 ^o ;
$\bar{p}p$	11.9 ^o ;
Slope (20 points)	
$\bar{p}p$	13.0–69.9 ^p ;
$p\bar{p}$	

^a Reference 10.
^b Reference 5.
^c Reference 4.
^d Reference 11.
^e Reference 12.
^f Reference 13.
^g Reference 2.
^h Reference 14.
ⁱ Reference 6.

^j Reference 15.
^k Reference 7.
^l By Re/Im we mean the ratio of the real to the imaginary part of the forward scattering amplitude.
^m Reference 16.
ⁿ Reference 17.
^o Reference 18.
^p Reference 3.

where $\nu = (s-u)/4M^2$ and

$$\xi_i = -\pi^{-1} \{ \pm 1 + \exp[-i\pi\alpha_i(t)] \} \Gamma(1-\alpha_i(t)),$$

$$f_{ss}^i(t) = (1-t/4M^2) [b_s^i \exp(c_s^i t)]^2 g_{ss}^i,$$

$$f_{nn}^i(t) = \frac{-t/4M^2}{1-t/4M^2} [b_n^i \exp(c_n^i t)]^2 g_{nn}^i,$$

$$f_{sn}^i(t) = (-t/4M^2)^{1/2} b_s^i b_n^i \exp[(c_s^i + c_n^i)t] g_{sn}^i,$$

and the g 's are the various ghost-eliminating mechanisms which satisfy the equation $g_{ss}^i g_{nn}^i = (g_{sn}^i)^2$.

The signature factors ξ_i contain an extra factor of α in the numerator, which is compensated for in defining the ghost-eliminating factors; i.e., we have used the relation

$$(\pi\alpha)^{-1} \Gamma(1-\alpha) = [\sin\pi\alpha \Gamma(1+\alpha)]^{-1}.$$

The units of the Φ 's are mb GeV/c, so the b 's are in (mb GeV/c)^{1/2}, the c 's are in (GeV/c)⁻², and the expressions for the observables are

$$\sigma_T = p_{\text{lab}}^{-1} \text{Im}\Phi_1(t=0),$$

$$d\sigma/dt = (0.226/p_{\text{lab}})^2 \{ |\Phi_1|^2 + |\Phi_3|^2 + 2|\Phi_5|^2 \},$$

$$P = \frac{-2 \text{Im}[\Phi_5^*(\Phi_1 + \Phi_3)]}{(|\Phi_1|^2 + |\Phi_3|^2 + 2|\Phi_5|^2)},$$

$$\text{Re/Im} = \text{Re}\Phi_1(t=0)/\text{Im}\Phi_1(t=0),$$

$$\text{slope} = \left[\ln \frac{d\sigma}{dt} (t = -0.064) - \ln \frac{d\sigma}{dt} (t = -0.065) \right] / 0.001.$$

The factor $0.226 = (\text{mb})^{1/2} \text{GeV}/4(\pi)^{1/2} \hbar c$ is the usual conversion factor to mb/GeV² for the DCS, including an extra constant factor $(16\pi)^{-1/2}$.

These expressions are equivalent to those used in RRCP except for the factor of 2 in the expression for the polarization (which was inadvertently omitted in writing the formula in that paper, but not in their calculation).

The ghost-eliminating factors appropriate for this form of ξ_i are

	Sense	Chew	Gell-Mann	No compensation
g_{ss}	$1/\alpha$	1	1	α
g_{nn}	α	α^2	1	α
g_{sn}	1	α	1	α

The kinematic factors differ from those given by Wang¹⁹ only in terms like $1-t/4M^2$, which are unimportant in the region of interest. We chose to retain the factors used in RRCP for comparison purposes.

IV. THREE-POLE FITS

A. General Features

In the spirit of RRCP,¹ the data were confronted with the simplest of Regge devices—viz., the three isoscalar trajectories P , P' , ω . Contributions from isovector exchange, such as π , ρ , and A_2 , can be estimated from the $n\bar{p}$ and $\bar{p}p$ charge-exchange cross sections to be smaller than the isoscalar contributions by at least an order of magnitude, and are ignored in this initial gambit for a simple representation of the data.

Because of the well-known factorization difficulty concerning the zero in the ω residue functions at the crossover point (see Sec. V), the ω contribution must be considered as representing an effective negative-parity amplitude which vanishes near $t = -0.13$ (GeV/c)² to account for the crossover phenomenon. The residues for the three-pole fits were parametrized by setting $b_{s,n}^{P,P'} = \text{const}$, $b_s^\omega = (1-t/t_0)^{1/2} \times \text{const}$, and $b_n^\omega = (1-t/t_0)^{1/2} \times \text{const}$, as required by factorization. Thus, the interpretation is that the P' and ω represent effective Regge contributions of positive and negative parity, respectively, while the P represents the Pomanchuk contribution. The deviation of the parameters from "canonical"²⁰ values then serves as some vague measure of the non-simple-Regge-pole content of the parametrization.

From the several varieties of parametrization tested, including various ghost-eliminating mechanisms and sign combinations of the helicity-flip residues, the following general features emerge:

(a) A generally good fit to all the $p\bar{p}$ DCS data, including the flattening seen in the 19.2- and 21.1-GeV/c data for $1.2 \leq -t \leq 2.3$ (GeV/c)²; (b) a concomitant inability to simultaneously reproduce the dips in the 8.0- and 16.0-GeV/c $\bar{p}p$ DCS near $t = -0.8$ (GeV/c)² (however, the fits for smaller $-t$ are generally good);

¹⁹ Ling-Lie C. Wang, Phys. Rev. **142**, 1187 (1966).

²⁰ By "canonical" trajectories we mean those which are linear and pass through the particles on a Chew-Frautschi plot. "Canonical" residue functions are those which best satisfy the CMSR and FESR for $K\bar{N}$ and πN .

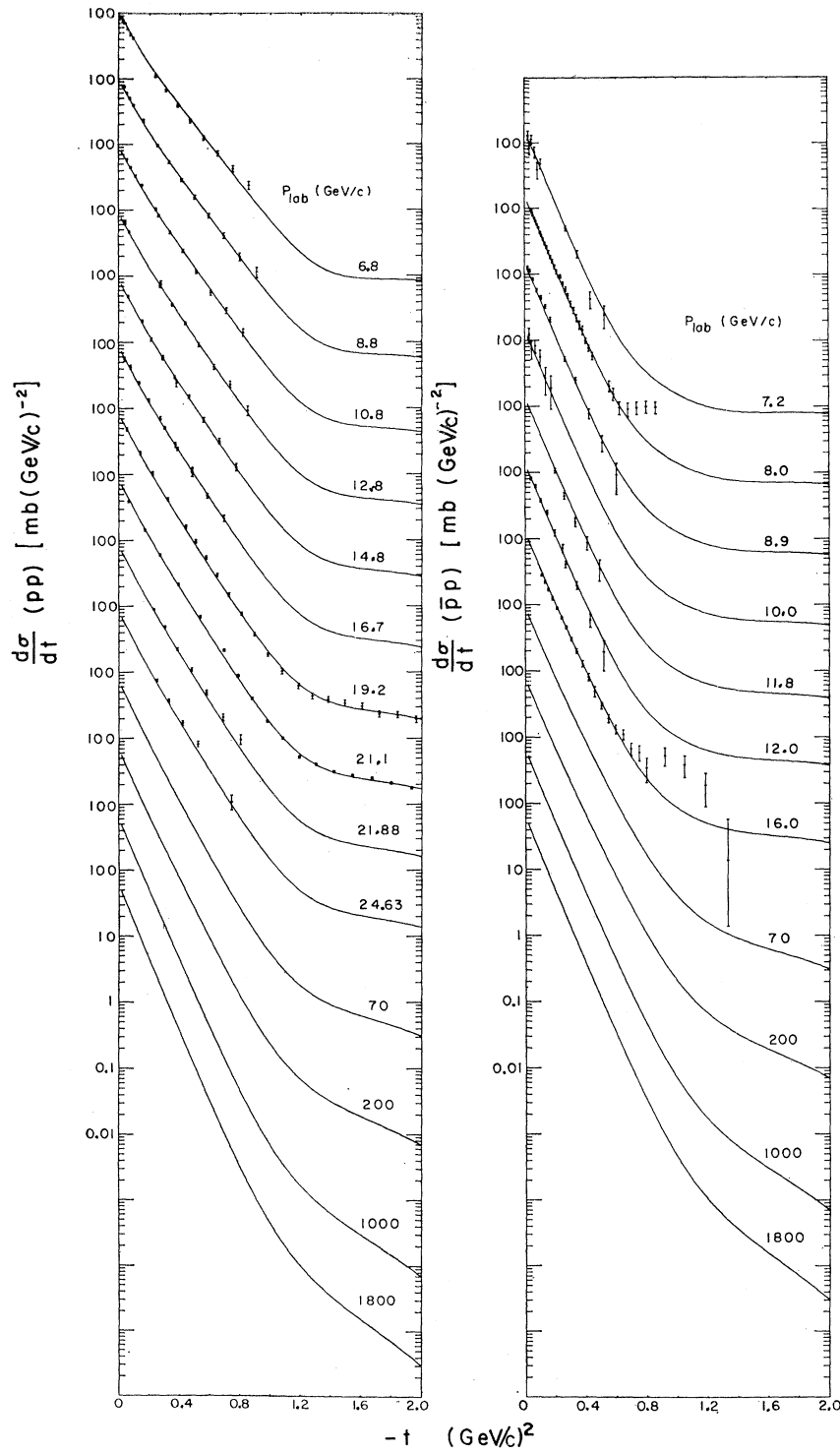


FIG. 1. pp and $\bar{p}p$ differential cross sections compared with three-pole fit 2 of Table II, with predictions to 1800 GeV/c . Successive sets of data are spaced by a decade.

(c) surprisingly good fits to the Serpukhov $p\bar{p}$ slope and $\bar{p}p$ total cross-section data, with a Pomeranchukon slope of about $0.35 (\text{GeV}/c)^{-2}$; and (d) polarization fits with χ^2 per point exceeding 2, but with vastly different shapes for different parametrizations.

These features were common to all parametrizations that produced reasonable fits (say, with χ^2 per point less than 2) to the data sample. The agreement for $-t < 0.6 (\text{GeV}/c)^2$ was very good—all the trouble is caused by large $-t$ structure.

B. Signs of Helicity-Flip Residue Functions

In terms of total χ^2 , the relative signs of the b_n 's could not be determined. Only in the shape of the polarization can one sign combination be distinguished from another. Although some combinations were able to reproduce the dip-bump structure of the 6.0-GeV/ c $p\bar{p}$ polarization data, none of the three-pole fits could reproduce the strong energy dependence seen for $-t > 1.0 (\text{GeV}/c)^2$, and all combinations gave a χ^2 of more than 2 per point for the polarization. Taking as a guideline that the three-pole parametrization should be able to reproduce the small $-t$ structure, such as the positive values for both $p\bar{p}$ and $\bar{p}p$ polarization and the dip near $-t = 0.6 (\text{GeV}/c)^2$, we fitted all the data except polarization with the various sign combinations and compared the predicted polarization from these parameters. The features found were [using the notation $\text{sgn}(b_n^P)$, $\text{sgn}(b_n^{P'})$, $\text{sgn}(b_n^\omega)$] as follows:

(a) When freed from the constraints of polarization fitting, all combinations wanted rather drastic small $-t$ behavior, presumably to match better the larger slope of the DCS data in that region. (b) Only the combinations $(+++)$, $(++-)$, $(-++)$, and $(-+-)$ give positive polarization for both $p\bar{p}$ and $\bar{p}p$ in the small $-t$ region. (c) The last two combinations, with $\text{sgn}(b_n^P) = -$, predict negative $p\bar{p}$ polarization for

TABLE II. Three-pole fit parameters for NVS parametrization. Fit 1 has only $\alpha_P = 1.0$ fixed; fit 2 has, in addition, $\alpha_{P'} = 1.0$ fixed.

		α_0	α'	b_s	c_s	b_n	c_n	t_0
Fit 1	P	1.0 ^a	0.35	5.8	1.6	0.97	-0.7	...
	P'	0.67	1.64	7.4	0.1	51.5	8.9	...
	ω	0.45	0.60	4.5	1.7	-31.0	3.5	0.13
Fit 2	P	1.0 ^a	0.36	5.8	1.6	1.0	-0.8	...
	P'	0.67	1.0 ^a	7.5	1.9	54.8	8.9	...
	ω	0.44	0.56	4.6	1.7	-25.4	3.7	0.13
		$d\sigma/dt$	σ_T	P	Re/Im^b	Slope	χ^2	No. of parameters
Fit 1		362	32	224	67	30	715	18
Fit 2		415	26	219	67	33	760	17
No. of data points		238	28	99	15	20	Total=400 data points	

^a Fixed.

^b Ratio of the real to the imaginary part of the forward scattering amplitude.

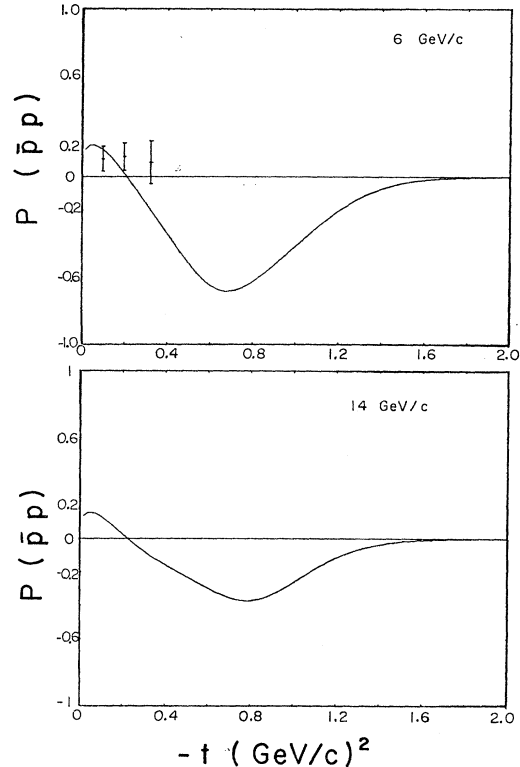


FIG. 2. $\bar{p}p$ polarization at 6 GeV/ c compared with three-pole fit 2 of Table II and a prediction at 14 GeV/ c .

$-t > 0.4 (\text{GeV}/c)^2$, contrary to fact. (d) The combinations $(+++)$ and $(++-)$ both seem to reproduce the general shape of the 6.0-GeV/ c data, including the large bump for $-t$ near $1.2 (\text{GeV}/c)^2$. From this we conclude that $\text{sgn}(b_n^P) = \text{sgn}(b_n^{P'}) = +$, that $\text{sgn}(b_n^\omega)$ is not well determined by this method, and that secondary contributions are necessary to reproduce the energy dependence seen in the large $-t$ polarization data.

Moreover, the conclusions seem to hold for the several combinations of ghost-eliminating mechanisms tried, as discussed in Sec. IV C.

C. Ghost-Eliminating Mechanisms

Recent analyses of low-energy πN^{21} and KN^{22} data using CMSR indicate that the mechanism preferred by P and P' in those reactions is the no-compensation mechanism, whereas the ω seems to prefer the sense-choosing mechanism. One observation can immediately be made—that is, if the P' contribution vanishes, as required by the no-compensation mechanism when $\alpha_{P'} = 0$, then the $\bar{p}p$ polarization at that point will be of opposite sign to the $p\bar{p}$ polarization and 5 to 10 times as large in the energy region considered here. This effect is due to the large antishrinking slope of the

²¹ V. Barger and R. J. N. Phillips, Phys. Rev. 187, 2210 (1969).

²² C. V. Dass and C. Michael, Phys. Rev. 175, 1774 (1968).

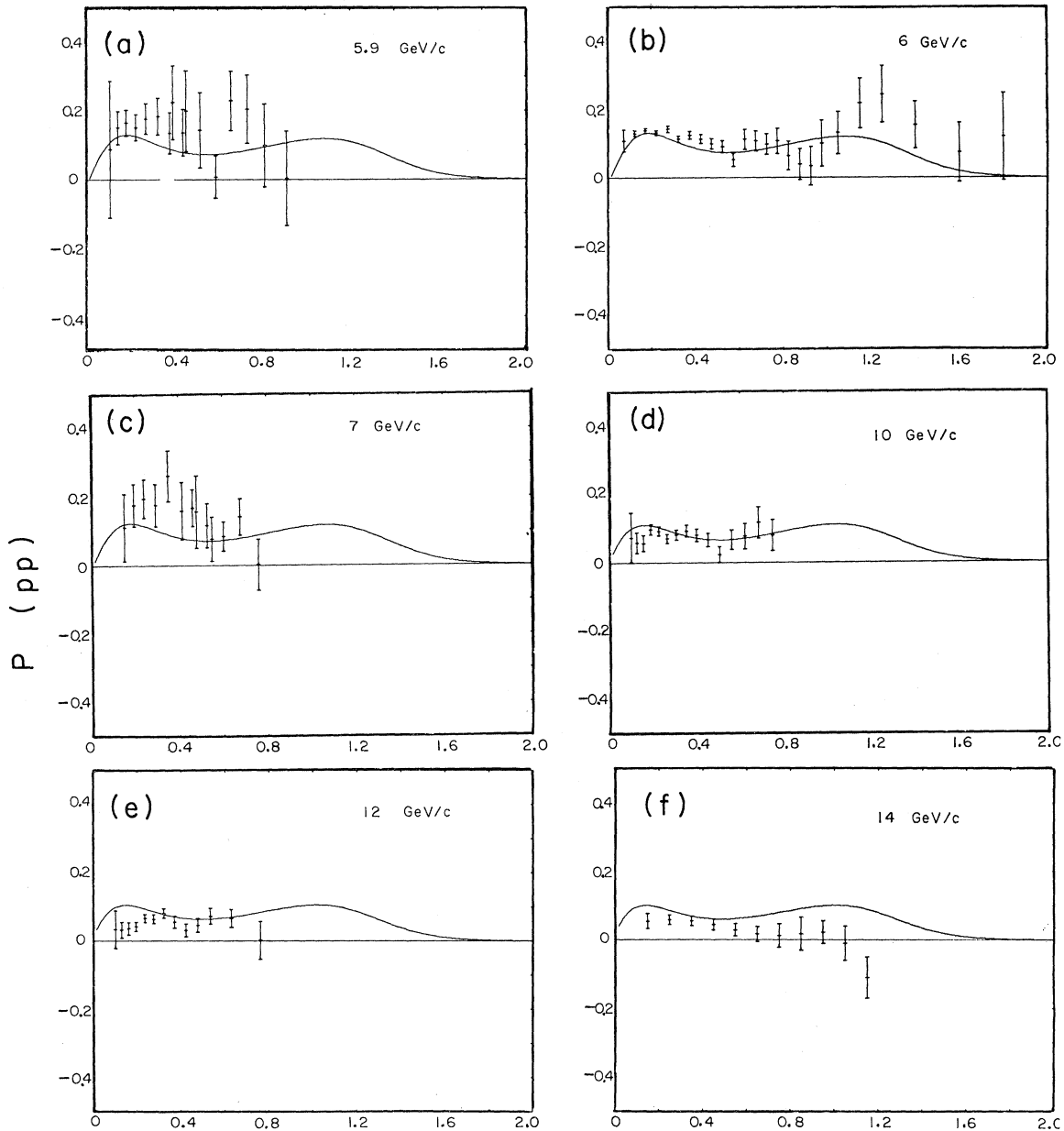


FIG. 3. $\bar{p}p$ polarization at (a) 5.9, (b) 6, (c) 7, (d) 10, (e) 12, and (f) 14 GeV/c compared with three-pole fit 2 of Table II.

$\bar{p}p$ DCS and to the fact that the ω contribution changes sign between the two expressions. If the dip in the $\bar{p}p$ data at $-t \approx 0.6$ (GeV/c) 2 is a reflection of $\alpha_{P'} = 0$, then $P_{\bar{p}p}$ at $p_{\text{lab}} = 6.0$ GeV/c and $-t \approx 0.6$ (GeV/c) 2 should be $-10 P_{pp}$ at the same point, which is 0.052 ± 0.019 —i.e., the non-compensation mechanism gives $P_{\bar{p}p} \approx -50\%$ there. Some data in this region would help determine whether the P' contribution should vanish or not, and thus help pin down the ghost-eliminating mechanism applicable to NN scattering.

Using the abbreviations S =sense choosing, C =Chew, G =Gell-Mann, and N =no compensation, we present a comparison of fits using several different combinations of ghost-eliminating mechanisms:

P	P'	ω	χ^2
N	N	S	715
N	N	C	708
C	C	S	778
G	G	G	732

From these results one can conclude that, although the

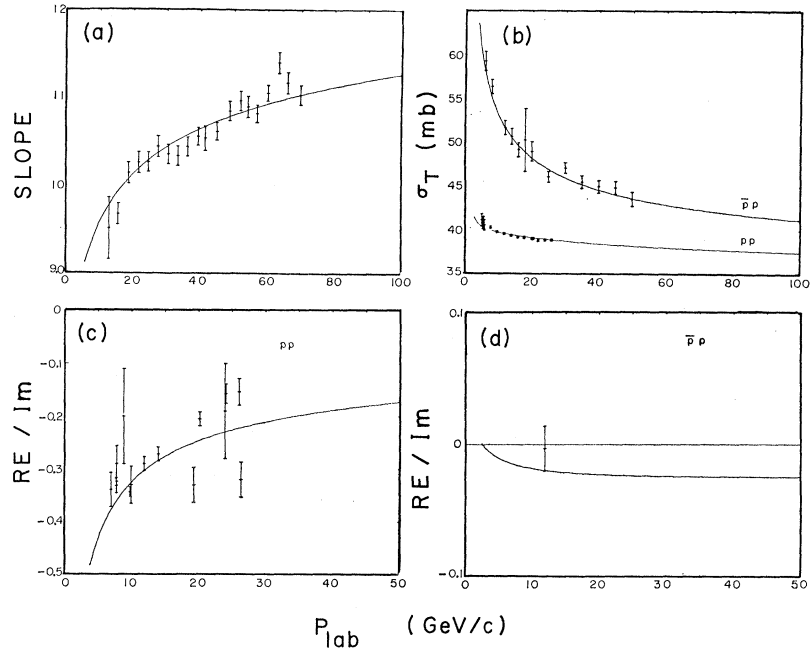


FIG. 4. Three-pole fit 2 of Table II compared with (a) slope of pp differential cross section, (b) total cross sections for pp and $\bar{p}p$, (c) the ratio of the real to imaginary part of the forward scattering amplitude for pp , and (d) the ratio of the real to imaginary part of the forward scattering amplitude for $\bar{p}p$.

vanishing of the P' seems to give a slightly better fit, the data really do not determine a mechanism. The parameters for the NNS fit, which agree with the features seen in CMSR and FESR applied to πN^{21} and KN^{22} data, were perhaps the most reasonable representation of all the data. It should also be noted that all these fits gave a similar prediction for $\bar{p}p$ polarization; i.e., $P_{\bar{p}p}$ is positive near the forward direction and large and negative ($\approx -50\%$) around $-t=0.6$ (GeV/c)². In the case of the NNS and NNC fits, it seems reasonable that the vanishing of the P' contribution, where $\alpha_{P'}=0$, leads to P - ω interference of equal and opposite magnitude. Since $d\sigma/dt$ for $\bar{p}p$ is on the order of only one fifth to one tenth of that for pp , the $\bar{p}p$ polarization should be 5 to 10 times as large in magnitude as the pp polarization. This must happen in any three-pole fit in which the P' contribution vanishes. However, it is somewhat of a mystery why the CCS and GGG fits, in which the P' contribution does not vanish, have structure very similar to the NNC and NNS fits. The phase cancellations must be somehow demanded by the data in such a way as to produce effective cancellation of the P - P' terms near $-t=0.6$ (GeV/c)².

In Table II we have presented two examples of three-pole fits, both of the NNS variety—i.e., the P and P' have the no-compensation mechanism and the ω has the sense-choosing mechanism. Fit 1 has only the P intercept fixed (at 1.0), and fit 2 has, in addition, the slope of the P' fixed at 1.0. In both fits, the ω trajectory emerged as rather flat, indicating that the difference between pp and $\bar{p}p$ data falls off somewhat more slowly at large $-t$ than a canonical ω trajectory would allow. The second fit is shown in Figs. 1–4, where it is seen that the $\bar{p}p$ DCS at $-t \approx 0.8$ (GeV/c)² is inade-

quately represented, as is the large $-t$ energy dependence of the polarization. Other features seem to be reasonably fitted.

V. FOUR-POLE FITS

A. General Features

The factorization problems associated with the incorporation of a universal zero in the ω residue func-

TABLE III. Parameters for four-pole fits of the form $\Phi = \Phi_P + \Phi_{P'} + \Phi_\omega + \Phi_{\omega'}$. In all fits the P and P' have the no-compensation mechanism and the ω and ω' have the sense-choosing mechanism.

		α_0	α'	b_s	c_s	b_n	c_n
Fit 1	P	1.0 ^a	0.32	6.0	1.7	3.3	0.3
	P'	0.63	0.98	7.4	8.7	56.6	2.7
	ω	0.49	0.53	4.3	0.5	-125.1	8.0
	ω'	0.58	0.74	10.4	1.0	9.1	0.0
Fit 2	P	1.0 ^a	0.31	5.5	1.7	3.1	0.3
	P'	0.70	1.20	7.6	2.0	38.1	3.6
	ω	0.39	1.0 ^a	5.0	1.3	-7.0	0.0
	ω'	0.39	0.5 ^a	12.9	1.8	30.9	0.6
Fit 3	P	1.0 ^a	0.37	6.2	1.8	2.6	-0.1
	P'	0.5 ^a	0.9 ^a	9.1	8.9	74.0	2.7
	ω	0.5 ^a	0.9 ^a	4.1	-0.3	-123.0	7.8
	ω'	0.5 ^a	0.9 ^a	11.5	0.6	2.0	-0.9
	$d\sigma/dt$				Re/Im	Slope	No. of χ^2 parameters
Fit 1	335	39	102	64	36	576	23
Fit 2	333	32	236	69	39	709	21
Fit 3	403	59	134	68	39	703	17
No. of data points	238	28	99	15	20	Total=400 data points	

^a Fixed.

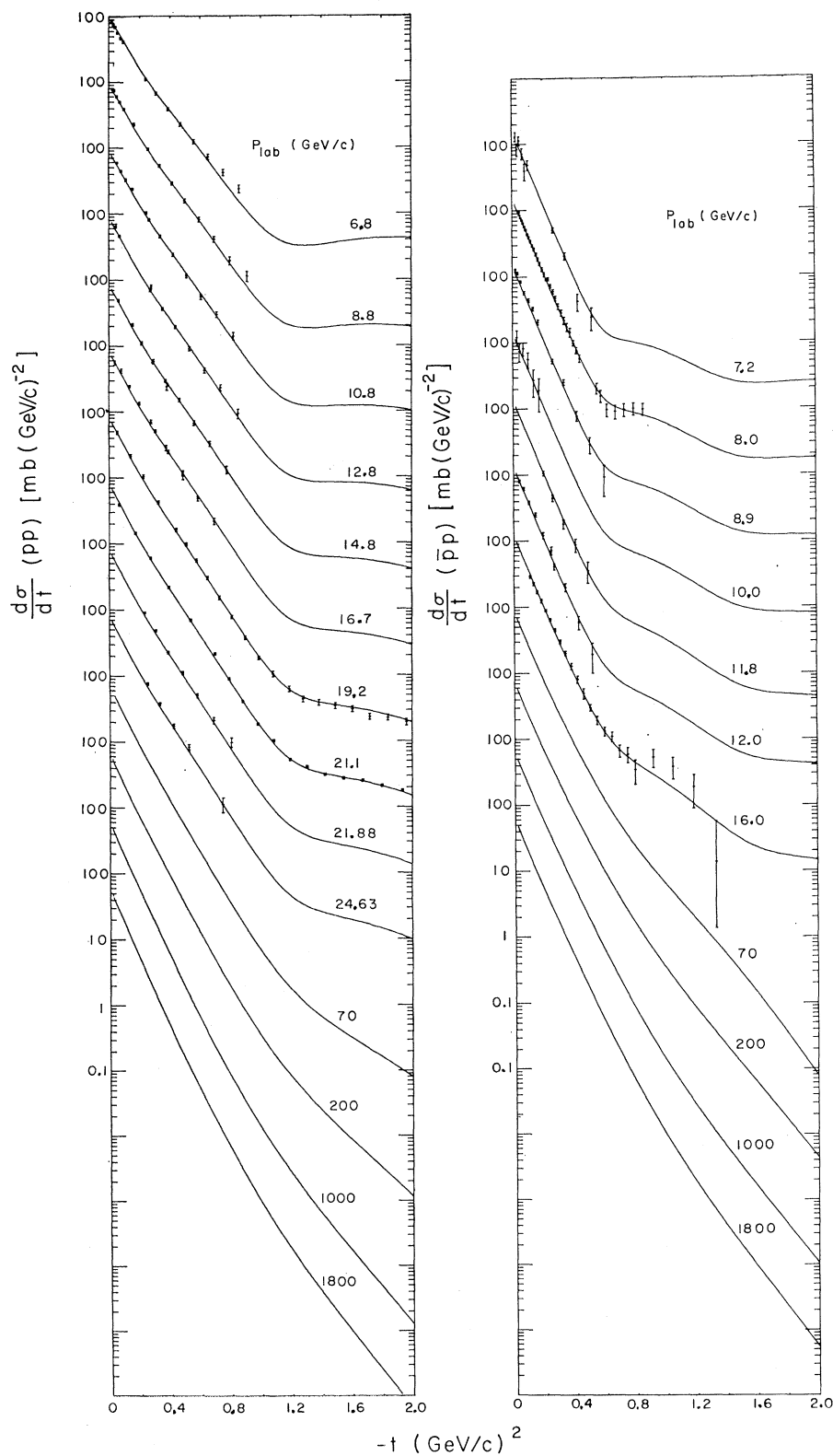


FIG. 5. pp and $\bar{p}p$ differential cross sections compared with four-pole fit 2 of Table III, with predictions to 1800 GeV/c. Successive sets of data are spaced by a decade.

TABLE IV. Parameters for four-pole fits of the form $\Phi = \Phi_P + \Phi_{P'} + \Phi_\omega + \Phi_{\omega'}$. In all fits the P and P' have the no-compensation mechanism and the ω and ω' have the sense-choosing mechanism.

	α_0	α'	b_s	c_s	b_n	c_n	
Fit 1	P	1.0 ^a	0.30	5.6	1.8	2.3	0.1
	P'	0.71	1.03	7.3	6.4	54.7	3.8
	ω	0.60	1.15	5.9	1.9	-35.8	1.2
	ω'	0.70	0.92	3.9	0.4	5.1	-0.6
Fit 2	P	1.0 ^a	0.29	5.7	1.9	3.0	0.4
	P'	0.67	0.97	7.7	4.7	62.1	4.3
	ω	0.41	1.0 ^a	8.2	1.5	-13.2	0.5
	ω'	0.40	0.5 ^a	6.6	1.0	28.0	0.4
Fit 3	P	1.0 ^a	0.38	6.2	1.8	2.5	-0.1
	P'	0.5 ^a	0.9 ^a	9.1	9.5	87.8	2.9
	ω	0.5 ^a	0.9 ^a	8.3	1.4	-77.2	9.2
	ω'	0.5 ^a	0.9 ^a	7.2	0.5	3.4	-0.9

	$d\sigma/dt$	σ_T	P	Re/ Im	Slope	χ^2	No. of parameters
Fit 1	302	20	175	57	34	588	23
Fit 2	305	32	222	67	35	661	21
Fit 3	421	56	152	74	43	746	17

No. of data points	238	28	99	15	20	Total = 400 data points	
--------------------	-----	----	----	----	----	-------------------------	--

^a Fixed.

tions are well known. This zero, which explains the crossover in DCS for $p\bar{p}$ and $\bar{p}p$, as well as for K^+p and K^-p , does not appear in $\pi N \rightarrow \rho N$,²³ or in $\gamma p \rightarrow \pi^0 p$,²⁴ as factorization requires. Thus there must exist

TABLE V. Parameters for various forms of five-pole fits. The $NNSS$ and $GGGG$ refer to the ghost-eliminating mechanisms, and the form of the amplitudes is indicated for each fit.

	α_0	α'	b_s	c_s	b_n	c_n	
Fit 1, $NNSS$, ($P+P'+P''$ $+\omega+t\omega'$)	P	1.0 ^a	0.26	6.0	2.0	2.1	0.0
	P'	0.65	1.0 ^a	7.1	6.5	72.0	10.3
	P''	-0.21	0.5 ^a	15.1	2.7	-98.0	2.6
	ω	0.52	1.0 ^a	4.3	5.5	-88.8	1.6
	ω'	0.38	0.5 ^a	9.0	1.4	19.4	0.6
Fit 2, $NNSS$, ($P+P'-P''$ $+\omega-\omega'$)	P	1.0 ^a	0.36	5.8	1.6	1.3	-0.5
	P'	0.60	0.9 ^a	9.9	3.5	71.3	5.4
	P''	0.34	0.5 ^a	9.9	0.5	38.5	8.1
	ω	0.41	0.9 ^a	9.6	1.6	-29.5	1.7
	ω'	0.40	0.5 ^a	8.4	1.3	20.5	0.3
Fit 3, $GGGG$, ($P+P'-P''$ $+\omega-\omega'$)	P	1.0 ^a	0.25	5.7	2.0	1.1	-0.2
	P'	0.68	0.9 ^a	6.2	6.2	51.2	5.9
	P''	-0.21	0.5 ^a	3.0	-0.3	-4.5	-0.8
	ω	0.45	0.9 ^a	14.0	1.0	-29.6	1.5
	ω'	0.45	0.5 ^a	11.9	1.3	2.9	0.4

	$d\sigma/dt$	σ_T	P	Re/ Im	Slope	χ^2	No. of parameters
Fit 1	286	18	82	69	47	502	25
Fit 2	308	24	144	63	40	579	25
Fit 3	303	25	124	61	46	561	25

No. of data points	238	28	99	15	20	Total = 400 data points	
--------------------	-----	----	----	----	----	-------------------------	--

^a Fixed.

²³ A. P. Contogouris, J. Tran Thanh Van, and H. J. Lubatti, Phys. Rev. Letters 19, 1352 (1967).

²⁴ P. di Vecchia, F. Drago, and M. Paciello, Nuovo Cimento 55A, 809 (1968).

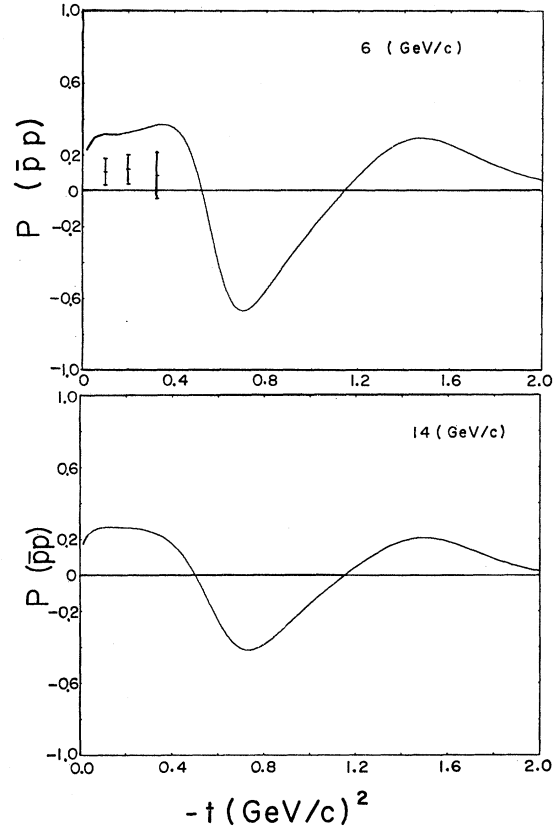


FIG. 6. $\bar{p}p$ polarization at 6 GeV/c compared with four-pole fit 2 of Table III and a prediction at 14 GeV/c.

another contribution to the same amplitudes, the ω' , to circumvent these problems as well as the disagreement between the analyses of $\pi N \rightarrow \rho N$ ²³ and KN FESR^{22,25} on the existence of a nonsense zero in the helicity-flip coupling at $-t=0.5$ (GeV/c)².

To obtain the zero in the negative-parity amplitudes as a cancellation between two Regge poles, ω and ω' , we considered two forms: (a) $\Phi_\omega + t\Phi_{\omega'}$ and (b) $\Phi_\omega - \Phi_{\omega'}$. It is evident that the cancellation zero will be energy dependent unless $\alpha_\omega(t) = \alpha_{\omega'}(t)$, and a cursory analysis of the data convinces one that only a very mild energy dependence of the crossover point in KN and NN DCS will be tolerated by the data. In general, we found that $\alpha_\omega(0) \approx \alpha_{\omega'}(0)$ was a necessity, whereas some difference in slopes was possible. Also, the four-pole fits were able to fit the shoulder in the $\bar{p}p$ DCS while simultaneously fitting the rest of the data as well as or better than the three-pole fits. Hence we conclude that the introduction of an ω' contribution, required *a priori* by factorization, provides a reasonable fit to all the $p\bar{p}$ and $\bar{p}p$ elastic data above $p_{lab} = 6.0$ GeV/c and for $-t < 2.5$ (GeV/c)². However, we must also conclude that uniqueness is not a quality of these

²⁵ G. V. Dass, C. Michael, and R. J. N. Phillips, Nucl. Phys. B9, 549 (1969).

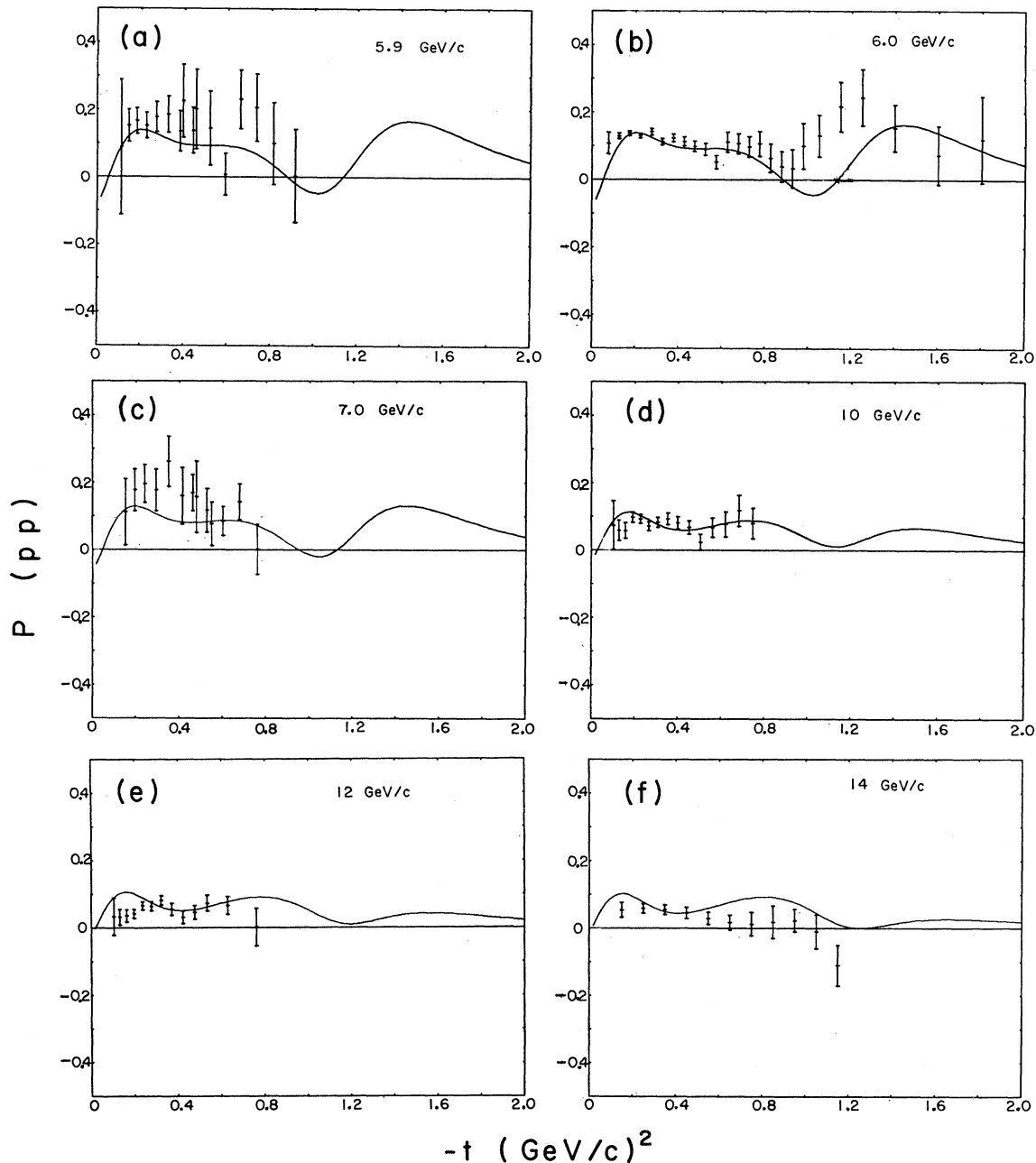


FIG. 7. pp polarization at (a) 5.9, (b) 6, (c) 7, (d) 10, (e) 12, and (f) 14 GeV/c compared with four-pole fit 2 of Table III.

fits any more than it was for the three-pole case. Adequate fits were obtained with either form (a) or (b), and with trajectories fixed to resemble cuts or fixed to enforce weak exchange degeneracy between the P' and ω . The best fits, in terms of minimum χ^2 , have rather perplexing parameters which tend to obscure rather than enlighten. All fits discussed below have the no-compensation mechanism for P and P' and the sense-choosing mechanism for the ω and ω' .

B. $\Phi_\omega + t\Phi_{\omega'}$

In Table III we display the parameters for three different fits having the form $\Phi = \Phi_P + \Phi_{P'} + \Phi_\omega + t\Phi_{\omega'}$. Fit 1 has only $\alpha_P(0) = 1.0$ fixed, and gives $\chi^2/N = 576/400$, considerably better than the three-pole fit. A physical interpretation of the ω and ω' trajectories would certainly be entertaining, but we are unprepared to speculate at present.

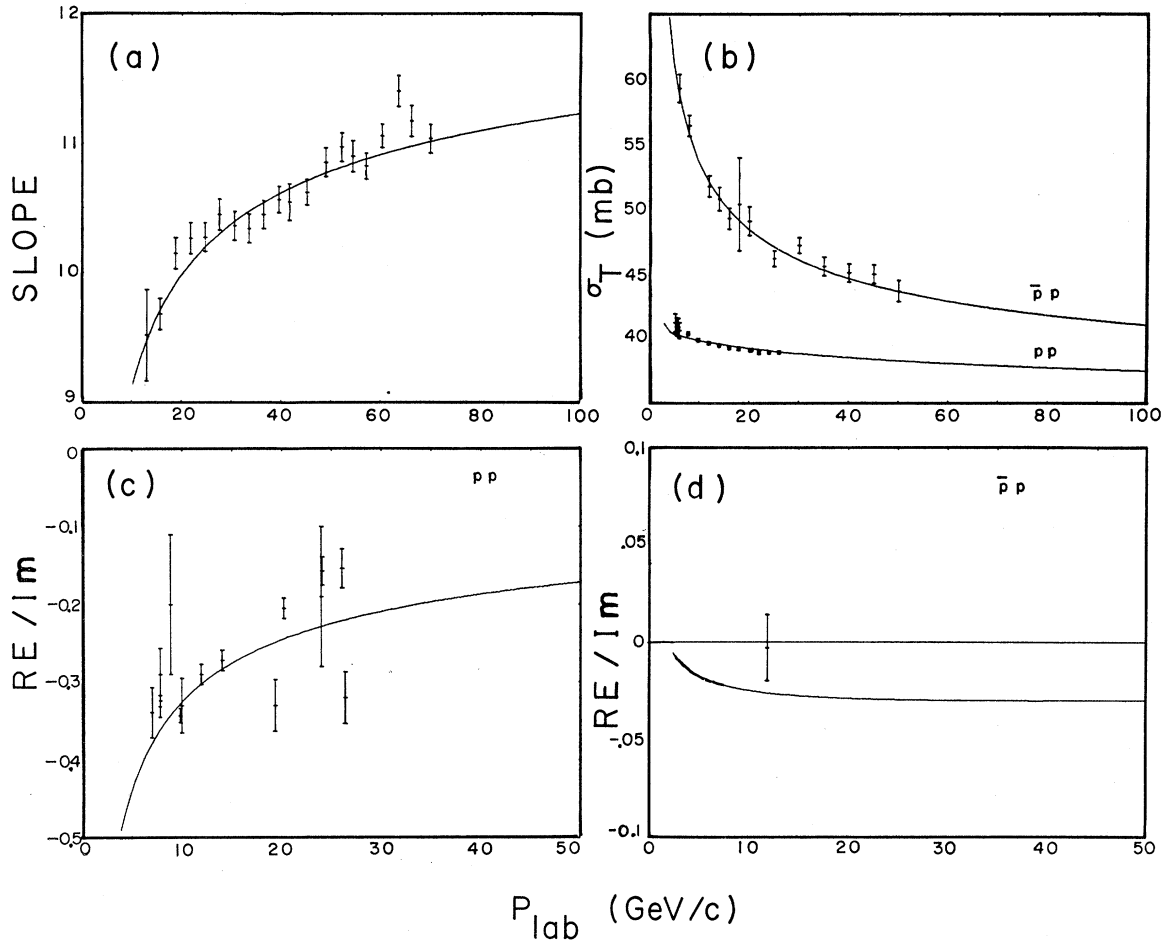


FIG. 8. Four-pole fit 2 of Table III compared with (a) slope of pp differential cross section, (b) total cross sections for pp and $\bar{p}p$, (c) the ratio of the real to imaginary part of the forward scattering amplitude for pp , and (d) the ratio of the real to imaginary part of the forward scattering amplitude for $\bar{p}p$.

Fit 2 has $\alpha_{\omega'}=1.0$ and $\alpha_{\omega''}=0.5$ fixed in addition, which allows a possible interpretation of the ω' as a P - ω cut (ignoring the $\ln s$ behavior, of course). This seems to have mainly spoiled the polarization fit, jacking up χ^2 to 709.

Finally, fit 3 has $\alpha_{\omega}(t)=\alpha_{\omega'}(t)=\alpha_{\omega''}(t)=0.5+0.9t$, and gives $\chi^2=703$. Thus the cut interpretation (fit 2) certainly is not forced upon us by this data. Some interpretations of two ω 's with the same trajectories appearing in NN scattering exist, but these are better left to their proponents for publicity. We simply state here that the data are compatible with such an interpretation.

C. $\Phi_{\omega}-\Phi_{\omega'}$

In Table IV are displayed the parameters for fits having the form

$$\Phi=\Phi_P+\Phi_{P'}+\Phi_{\omega}-\Phi_{\omega'}.$$

This is the simplest form for producing a cancellation, and is perhaps easier to interpret in terms of dipoles,

cuts, or something worse. As before, we give the reader three choices of trajectories to speculate upon; as before, the results are similarly confusing.

Fit 1 has only the P intercept fixed and the results seem fairly close to exchange degeneracy for the trajectories. The χ^2 of 588 is competitive with that in Sec. V B, and there is little to distinguish between the two forms in the results.

Fit 2 has $\alpha_{\omega'}=1.0$ and $\alpha_{\omega''}=0.5$, which pushes the χ^2 up to 661, mainly due to the polarization fit. This is the fit displayed in Figs. 5-8, where it can be seen that all the data are adequately represented by a four-pole fit with reasonable values of the parameters.

Fit 3 with degenerate trajectories is equivalent to breaking factorization for the ω , and simultaneously including more complicated residue functions. In this fit, $\Phi_{\omega^{ss}}-\Phi_{\omega'^{ss}}=0$ at $t=-0.17$ (GeV/c) 2 , $\Phi_{\omega^{nn}}-\Phi_{\omega'^{nn}}=0$ at $t=-0.31$ (GeV/c) 2 , and $\Phi_{\omega^{sn}}-\Phi_{\omega'^{sn}}\neq 0$. This is in qualitative agreement with the KN FESR results, 22 in which the nonflip coupling seems to vanish at a different value of t from that of the flip coupling.

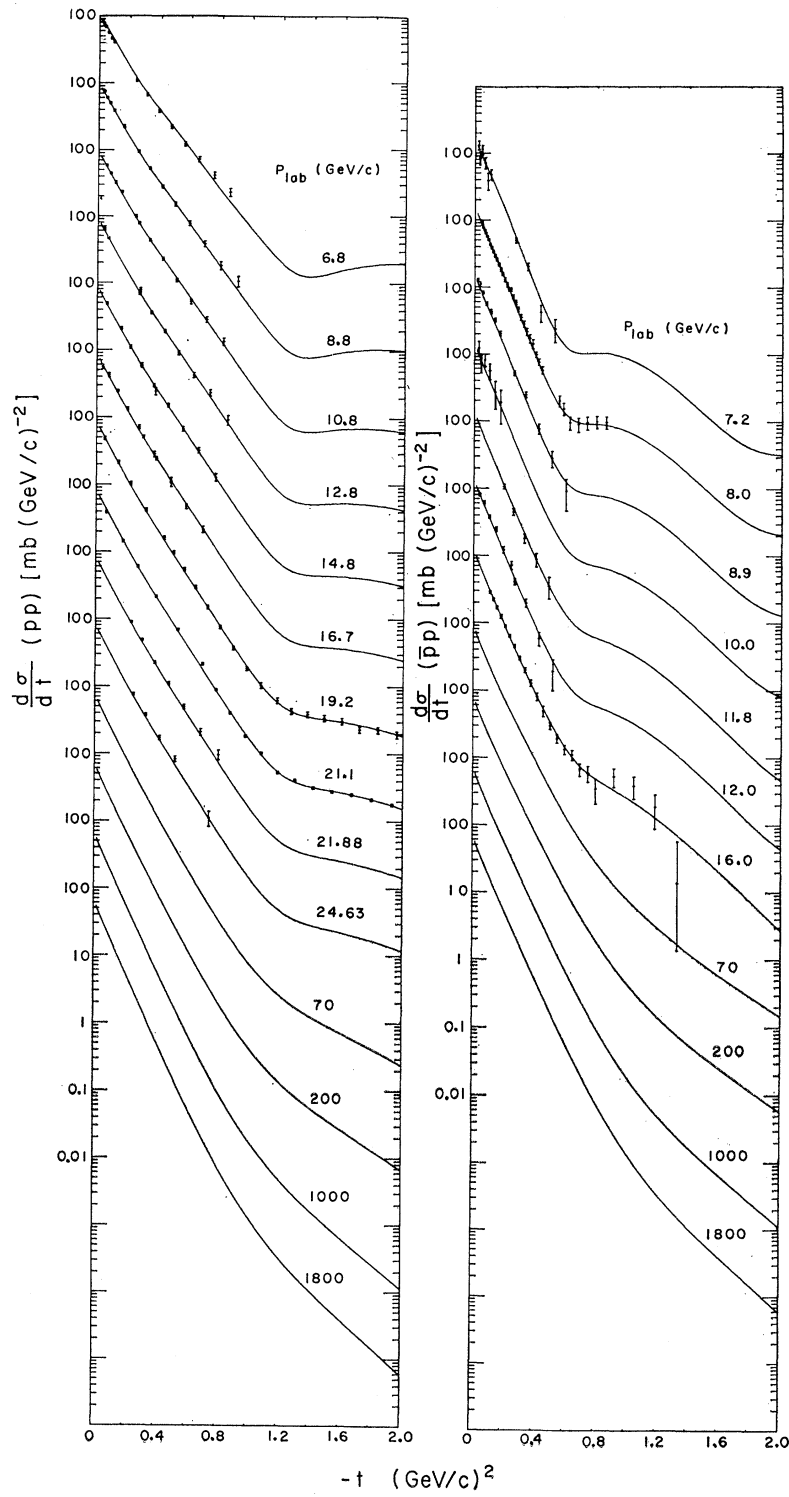


FIG. 9. pp and $\bar{p}\bar{p}$ differential cross sections compared with five-pole fit¹ of Table V, with predictions to 1800 GeV/c . Successive sets of data are spaced by a decade.

D. Summary

The tables of parameters are meant to illustrate the nonuniqueness of Regge fits of NN elastic data as well as the adequacy of the Regge-pole representation. There need to be further restrictions on the residue functions, such as those provided by sum rules for πN and KN scattering. The relation $A' \approx \nu B$, predicted by sum rules for P and P' ,^{21,22} should, by factorization, imply the relations

$$\begin{aligned} b_s^P \exp(c_s^P t) &\approx b_n^P \exp(c_n^P t), \\ b_s^{P'} \exp(c_s^{P'} t) &\approx b_n^{P'} \exp(c_n^{P'} t). \end{aligned}$$

For the four-pole fits the relation is fairly well satisfied for the P , but not for the P' .

For completeness, some fits were tried with the $1-t/t_0$ factor in the ω amplitudes; i.e., the form $(1-t/t_0)\Phi_\omega + \Phi_{\omega'}$ was used. This form was apparently unable to reproduce the structure in the $\bar{p}p$ DCS and was therefore not investigated further.

VI. FIVE-POLE FITS

Since the sum-rule calculations²¹ seem to require yet another vacuum contribution, dubbed the P'' , some varieties of five-pole fits were tried. As expected, such a parametrization leads to rampant ambiguity, and the only way to obtain results with even a modicum of interest is to fix some of the trajectory parameters. We define a trajectory with (a) a slope near $0.5 (\text{GeV}/c)^{-2}$, (b) whose amplitude occurs with a negative sign relative to like contributions, to be "cutlike" (as opposed to the usual, or "polelike" parametrization). Symbolically, a fit with the P'' and ω' treated as cutlike will be indicated by $P+P'-P''+\omega-\omega'$, etc. In general, the five-pole fits gave $\chi^2 < 600$, and most varieties of parametrization produced fits which were indistinguishable from the others. The ω' preferred to remain cutlike, as it must in order to provide the weakly energy-dependent crossover zero in the DCS. The P'' gave equally good fits with cutlike or polelike parameters. These statements refer to fits in which the slopes of P' and ω were held fixed at 0.9 or 1.0. In Table V we list some parameters as examples of five-pole fits. We emphasize that there is nothing unique about these parameters—there exist many other sets that produce adequate fits to the data, including cutlike forms as well as polelike forms, various ghost-eliminating mechanisms, and other variations. For example, residue functions of the form $\beta = \exp(-0.5i\pi\alpha)[b \exp(ct)]$ produced fits competitive with the Γ -function forms in Sec. III.

Fit 1 in Table V has the form $P+P'+P''+\omega+tw'$, with the vacuum poles all having the no-compensation mechanism and the ω 's having the sense-choosing mechanism. The P intercept and the slopes of the other poles were held fixed. This fit is shown in Figs. 9–12.

Fit 2 has the form $P+P'-P''+\omega-\omega'$, and has the same ghost eliminators as fit 1. The difference of 77 in χ^2 is probably not significant.

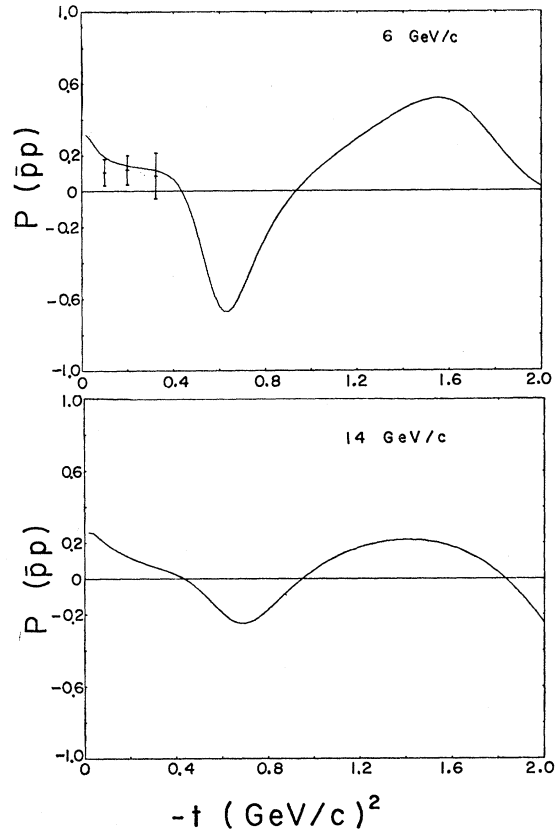


FIG. 10. $\bar{p}p$ polarization at 6 GeV/c compared with five-pole fit 1 of Table V and a prediction at 14 GeV/c.

Fit 3 also has the form $P+P'-P''+\omega-\omega'$, but here all poles have the Gell-Mann ghost-eliminating mechanism. The difference between the fits is noticeable only in the prediction of the $\bar{p}p$ polarization, which is somewhat larger for small $-t$ and smaller in magnitude for intermediate $-t$ for this parametrization than for the others. However, since the data are hardly sufficient to determine the behavior in this region, no preference can be voiced for any version of parametrization.

VII. DISCUSSION

In summary several points of interest emerge.

(1) The three-pole parametrization is inadequate, mainly because of the failure to fit the structure in the $\bar{p}p$ DCS.

(2) The four-pole parametrization, even when restricted to a factorization-breaking form that really only need involve the addition of one additional parameter over the three-pole form, is capable of giving a reasonable representation of all the data. However, the data, which are some of the best high-energy data in existence, do not distinguish between various possible parametrizations.

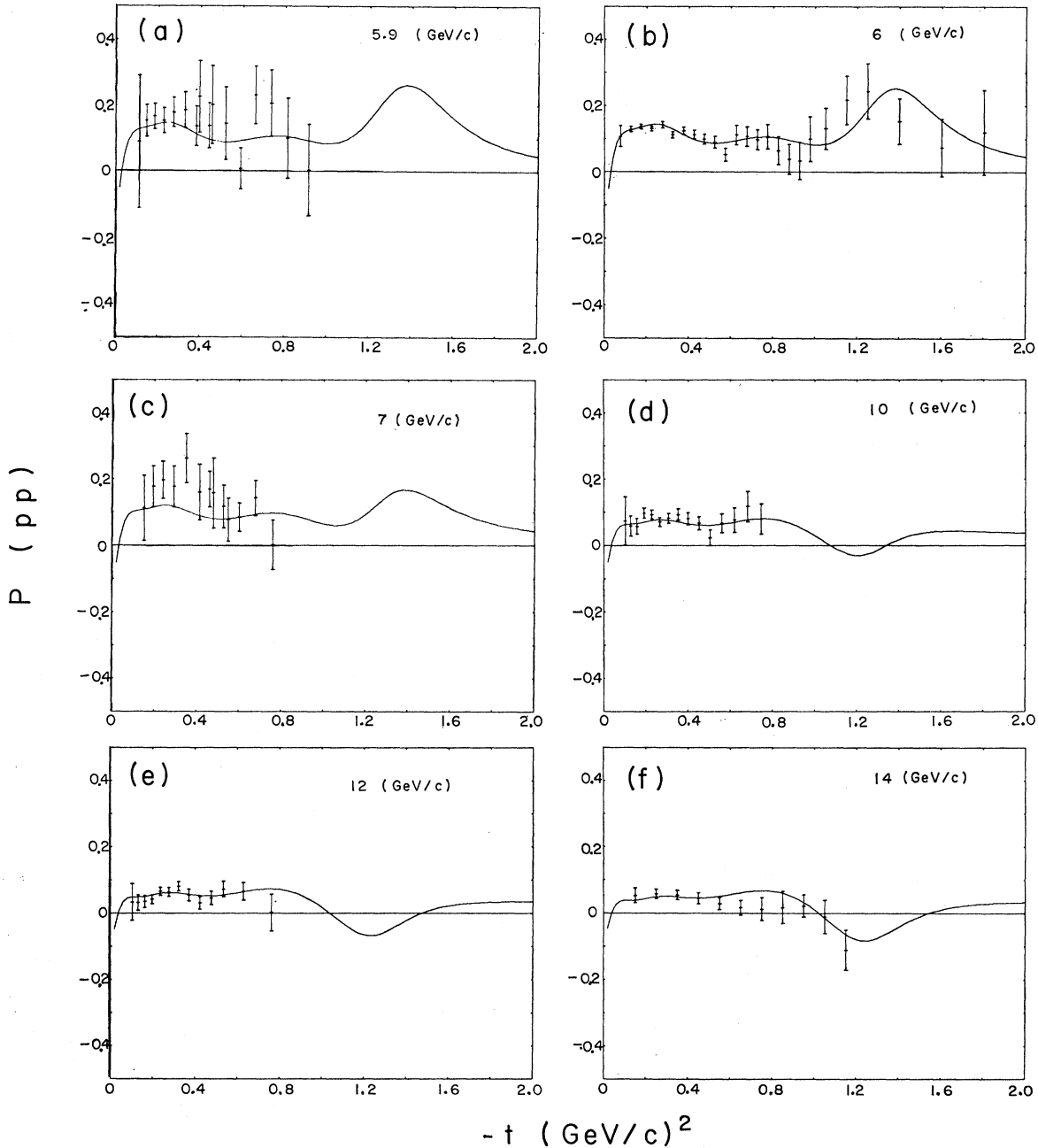


FIG. 11. pp polarization at (a) 5.9, (b) 6, (c) 7, (d) 10, (e) 12, and (f) 14 GeV/c compared with five-pole fit 1 of Table V.

(3) Five-pole fits, without the use of sum rule constraints, are nonunique and probably not very useful.

Some fits were tried on a combination of $\pi^\pm p$ elastic and charge exchange, $K^\pm p$ elastic and charge exchange, and the above pp and $\bar{p}p$ elastic data, obtained by using the usual P , P' , ρ , A_2 , and ω and enforcing factorization. Our preliminary conclusions are that fits with $\chi^2/\text{point} \approx 3$ can be obtained to all the above data together with reasonable parameters. Incompatibility

of the many data sets involved seems to be more responsible for the bad fit than inadequacies of the simple Regge-pole model. Since it is very difficult to assure oneself that all these experiments have no normalization errors with respect to each other, factorization constraints do not seem to be the answer to obtaining unique fits. The most positive statement that can be made is that the present NN data certainly cause no embarrassment for simple Regge-pole theory (or for some other theories, for that matter).

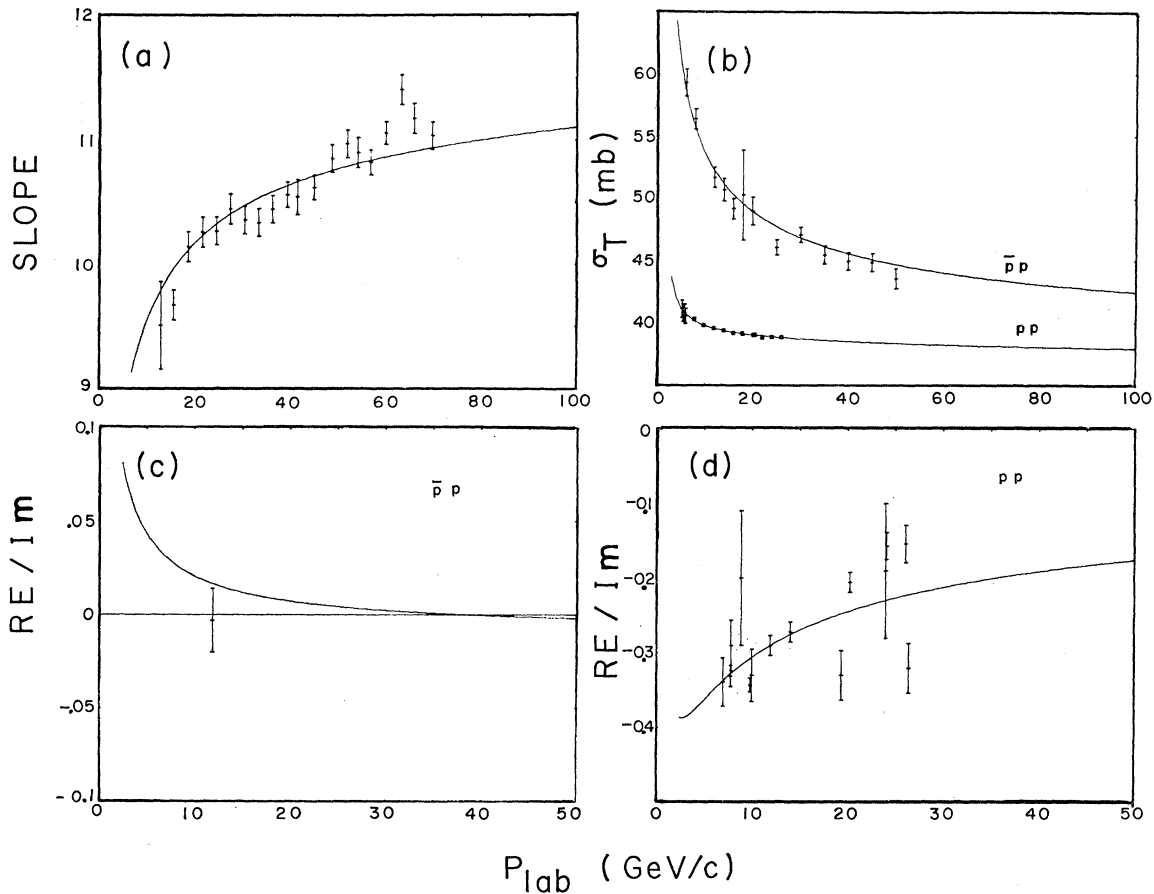


FIG. 12. Five-pole fit 1 of Table V compared with (a) slope of $p\bar{p}$ differential cross section, (b) total cross sections for $p\bar{p}$ and $\bar{p}p$, (c) the ratio of the real to imaginary part of the forward scattering amplitude for $\bar{p}p$, and (d) the ratio of the real to imaginary part of the forward scattering amplitude for pp .

As for predictions, very little should be said when a unique fit has not been found. Again, there is one positive statement that can be made from our experience—that is, if the P and P' choose the no-compensation mechanism, then a $\bar{p}p$ polarization prediction of around -50% near $t = -0.6$ (GeV/c)² seems unavoidable. Even though one can think of many ways of avoiding this (e.g., through ω - ω' interference), all good fits with this ghost-eliminating mechanism—three-pole, four-pole, and five-pole—produced the same prediction. This is bothersome mainly because of a parallel which can be drawn with the Kp data. At $p_{lab} = 2.0$ – 3.0 GeV/c , pp and $\bar{p}p$ as well as K^+p and K^-p have positive polarization for $-t < 0.8$ (GeV/c)².²⁶ At $p_{lab} = 6.0$ GeV/c , the K^+p and K^-p polarizations are still both positive in that t range, and the $\bar{p}p$ data are also positive for $-t < 0.3$ (GeV/c)². Hence one might expect the $\bar{p}p$ polarization to remain

²⁶ C. Daum, F. C. Erne, J. P. Lagnaux, J. C. Sens, M. Steuer, and F. Udo, Nucl. Phys. B6, 617 (1968).

positive for $t = -0.6$ (GeV/c)², as does the K^-p . If it should remain positive, we would face a drastic contradiction to all of the parametrizations in which the P' vanishes near $t = -0.6$ (GeV/c)². Fits in which the Gell-Mann mechanism was used (fit 3 in Table V) could predict positive $\bar{p}p$ polarization in that region, but this is apparently in contradiction to the CMSR results²¹ on the P' ghost-eliminating mechanism. Obviously, data in this region are needed to settle the question.

ACKNOWLEDGMENTS

We wish to thank Professor Geoffrey F. Chew and the Lawrence Radiation Laboratory for their hospitality. One of the authors (D. M. A.) wishes to thank the U. S. Atomic Energy Commission for support, and another (W. H. G.) wishes to thank the Air Force Office of Scientific Research and National Research Council for support. Also, the authors thank Professor G. Bellettini for providing some preliminary data.